RSC Advances

PAPER

View Article Online
View Journal | View Issue

Check for updates

Cite this: *RSC Adv.*, 2022, **12**, 31402

# In-depth drug delivery to tumoral soft tissues *via* pH responsive hydrogel

Shumaila Sarwar,[ab] Sajid Bashir,[b] Mulazim Hussain Asim,[b] Fakhera Ikram,[a] Arsalan Ahmed, *[a] Ume Omema,[a] Anila Asif,[a] Aqif Anwar Chaudhry,[a] Yong Hu [c] and Cem Bulent Ustundag[d]

A pH responsive nanoparticle–hydrogel hybrid drug delivery system was investigated for in-depth anticancer drug delivery to solid tumours. It consists of acid susceptible polymer nanoparticles loaded in a chitosan hydrogel. The hybrid formulation was characterized by UV-visible spectroscopy, FTIR, SEM, TEM, particle size analysis, zeta potential measurement and viscosity measurement. Drug encapsulation and nanoparticle loading efficiencies were found to be 48% and 72% respectively which describes the efficient interaction of the chemical entities in this hybrid drug delivery system. The hydrogel exhibited pH responsive behaviour: minimal drug and nanoparticle release at physiological pH but an increase in viscosity under acidic conditions and fast nanoparticle and drug release. The cytotoxicity of the drug loaded hydrogel was investigated against the MCF-7 breast cancer cell line along with the drug and nanoparticles without hydrogel. The drug loaded hydrogel showed a better cytotoxic effect on MCF-7 cancer cells. Thus, drug loaded nanoparticles containing hydrogel could be a better option for maximum drug distribution in tumours.

Received 7th September 2022
Accepted 26th October 2022

DOI: 10.1039/d2ra05639a

rsc.li/rsc-advances

Open Access Article. Published on 02 November 2022. Downloaded on 11/13/2022 8:39:19 PM.
This article is licensed under a Creative Commons Attribution-NonCommercial 3.0 Unported Licence.

## 1. Introduction

A solid tumour is an abnormal tissue accumulation that usually does not contain cysts and may be benign or malignant. It has a host of karyotypic changes that make it very difficult to establish the primary cytogenetic events.[1,2] The unusual growth of a tumour differs from normal tissue, and it changes the microenvironment of the tumour tissue, for example high interstitial fluid pressure (IFP), abnormal blood vessels, poor lymphatic drainage and dense extracellular matrix (ECM).[3–5] These characteristics of the tumour microenvironment act as a barrier for intratumoral drug delivery. Irregular tumour vasculature decreases the blood supply and entry of drugs into the tumour.[6] Dense ECM and high IPF hinder the in-depth penetration of drugs and distribute the drug in the periphery of the tumour and neighbouring healthy cells.[7] Low bioaccessibility of drugs to target solid tumours and rapid clearance can lead to inadequate therapy and increased incidence of drug resistance. Local administration of drugs demonstrates a better antitumour effect over systemic chemotherapy owing to highly selective accumulation in the tumour and active cellular uptake.[8] In this regard injectable hydrogels have exhibited prolonged drug release, high drug content at tumour site and low systemic toxicity.[9] However, such systems also have limited drug penetration in tumour tissue and cancer cells. Therefore, more efficacious, and smarter hydrogel-based drug delivery systems are required for desired penetration and accumulation of drug in tumour tissues and cells.

Hydrogels are comprised of cross-linked polymer networks that have a high number of hydrophilic groups. These networks have a high affinity for water but are prevented from dissolving due to the chemical or physical bonds formed between the polymer chains. Water penetrates these networks causing swelling and giving the hydrogel its form.[10] Fully swollen hydrogels have some physical properties common to living tissues, including low interfacial tension with biological fluids. The low interfacial tension between the hydrogel surface and body fluid minimizes protein adsorption and cell adhesion, which reduces the chances of a negative immune reaction.[11] In addition, hydrogels have several additive characteristics that make them excellent drug delivery vehicles. First, many polymers used in hydrogel preparations have mucoadhesive and bioadhesive characteristics that enhance drug residence time and tissue permeability. This adhesive property is due to interchain bridges between the functional groups of hydrogel and the mucus glycoproteins, which can help enhance site-specific binding.[11] Environmentally responsive hydrogels, for instance hydrogels for cancer treatment swell in response to external

[a]*Interdisciplinary Research Centre in Biomedical Materials, COMSATS University Islamabad, Lahore, Pakistan. E-mail: arsalanahmed@cuilahore.edu.pk*
[b]*College of Pharmacy, University of Sargodha, Sargodha, Pakistan*
[c]*Institute of Materials Engineering, National Laboratory of Solid State Microstructure, College of Engineering and Applied Sciences, Nanjing University, Nanjing, Jiangsu, China*
[d]*Department of Bioengineering, Faculty of Chemical and Metallurgical Engineering, Yildiz Technical University, Turkey*


© 2022 The Author(s). Published by the Royal Society of Chemistry

Open Access Article. Published on 02 November 2022. Downloaded on 11/13/2022 8:39:19 PM.
This article is licensed under a Creative Commons Attribution-NonCommercial 3.0 Unported Licence.

conditions, such as pH and temperature that effectively open the pores to enhance diffusion of the entrapped therapeutic agent under predetermined conditions. This type of controlled release is used to limit drug release outside of the effective range of the diseased tissue.[12] Although drug loaded hydrogel showed better drug release profile and drug activity, hydrophobic drug is less dispersed in hydrogel and rapid release of drug molecules is observed from hydrogel.[13]

Encapsulation of hydrophobic drug in amphiphilic polymeric nanoparticles and then loading in hydrogel could enhance the stability, dispersion and sustained release of drug.[14,15] Nanoparticles-hydrogel hybrid drug delivery system has received great attention. This system not only preserves the structural and physicochemical characteristics of nanoparticles but also provides additional features to strengthen overall therapeutic effect. Such properties cannot be obtained with single independent system.[16] Nanoparticles loaded hydrogels possess prolonged drug release duration due to involvement of two steps *i.e.*, nanoparticles release from hydrogel and then drug release from nanoparticles.[17] Stimuli responsive nanoparticle–hydrogel systems have received more attention due to intrinsic physicochemical and biological properties. These hydrogels are in limelight due to their simplicity, response to abnormal tumour microenvironment *e.g.* low pH and site specific release of encapsulated therapeutic cargo.[18] The synergism between stimuli responsive nanoparticles and hydrogel makes it highly responsive to tumour pathological environment and selective for cancer cells.

We worked on low pH responsive nanoparticles–hydrogel hybrid drug delivery system for better accumulation, penetration, and distribution of anticancer drug in tumour tissue (Fig. 1). For this, three amphiphilic copolymers with distinct properties were synthesized *i.e.*, polycaprolactone-polyethyleneimine (PCL-PEI) with acid responsive charge reversibility, polycaprolactone-polyethyleneimine-folate (PCL-PEI-folate) with specific targeting and polycaprolactone-polyethyleneimine-polyethylene glycol (PCL-PEI-PEG) with stealthy and acid labile linkages. These copolymers self-assembled in aqueous media to fabricate three layered nanoparticles. This outer layer consists of polyethylene glycol (PEG), makes nanoparticles stable and stealthy, and sheds off in tumour acidic environment to expose middle layer, which contain polyethyleneimine (PEI) for negative-to positive-charge reversal behaviour and folate for specific targeting. The inner layer is made of polycaprolactone (PCL) and acts as reservoir for anticancer hydrophobic drug. Later, these nanoparticles were loaded in chitosan hydrogel to fabricate acid sensitive nanoparticles–hydrogel hybrid drug delivery system. Thus, hydrogel efficiently retains the nanoparticles in physiological pH of healthy tissue due to attractive interactions between negatively charged nanoparticles and amines of chitosan. However, both amines of chitosan and nanoparticles are protonated at low pH (tumour microenvironment) to cause repulsion between chitosan chains and nanoparticles. Consequently, nanoparticles are released in tumour tissue. Now, stealthy outer layer of nanoparticles facilitates the well dispersion of nanoparticles in tumour mass and degrades to show middle targeting layer. It helps in in-depth penetration of nanoparticles in tumour tissue. Finally, the inner layer decomposes to release drug inside tumour cells.

## 2. Experimental section

### 2.1 Materials

Poly($\varepsilon$-caprolactone) (PCL) 45 kDa was purchased from Polysciences Asia Pacific, Taiwan, *N*,*N*′-dicyclohexylcarbodiimide

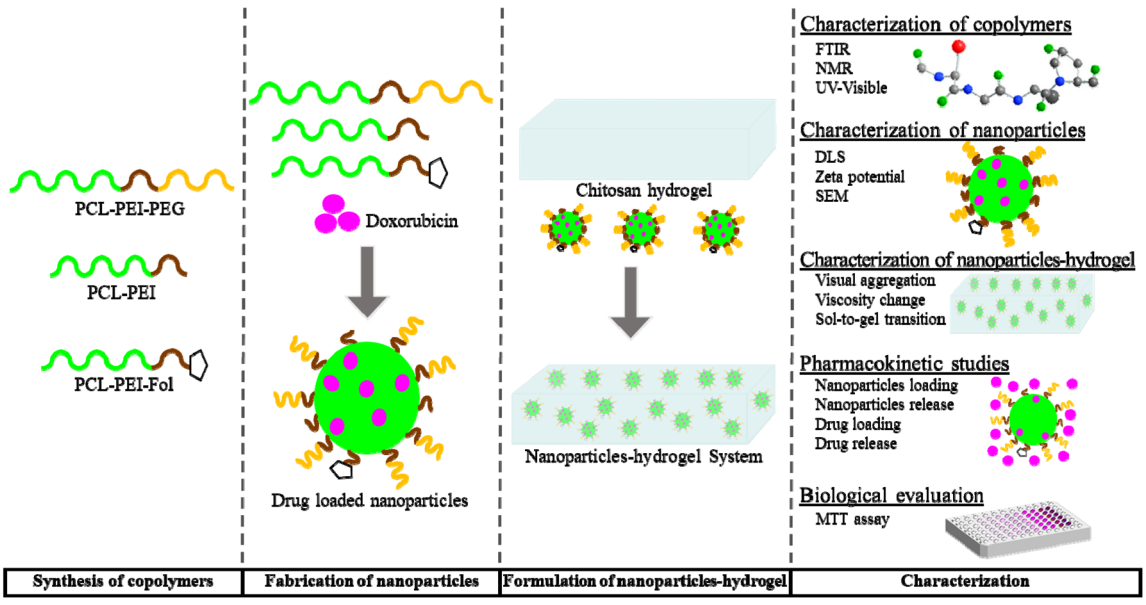



Fig. 1 Schematic illustration of formulation and characterization of nanoparticles–hydrogel drug delivery system.

Open Access Article. Published on 02 November 2022. Downloaded on 11/13/2022 8:39:19 PM.
This article is licensed under a Creative Commons Attribution-NonCommercial 3.0 Unported Licence.

and dichloromethane were obtained from Merck, Germany. Polyethyleneimine (PEI) 600 Da, glutaraldehyde, Dulbecco's modified eagle medium (DMEM) and tetrahydrofuran (THF) were purchased from Sigma-Aldrich, USA and *N*-hydroxysuccinimide (NHS), fetal bovine serum (FBS), penicillin/streptomycin and dialysis membranes (5, 10, and 15 kDa MWCO) were obtained from Thermo Fisher Scientific USA. Moreover, deionized water from Merck Millipore, USA, trypsin–EDTA solution from Invitrogen Life Technologies and doxorubicin HCl from LGM Pharma, USA was used. All other materials used in this research work were of analytical grade and used as received without further processing.

### 2.2 Synthesis of copolymers

For the fabrication of PCL-PEI and PCL-PEI-Fol copolymers, conjugation technique was applied as reported earlier with some modification.[19] In brief, 1.2 mM DCC and 1.2 mM NHS were mixed and stirred continuously for 30 min using magnetic stirrer. Then, 0.37 mM PCL solution in THF was added dropwise in above mixture and stirring was continued for 3.5 hours at 4 °C to acquire activated PCL. In the following, 0.4 mM PEI solution was added in activated PCL solution by continuous stirring for an hour. A white precipitate was formed that was filtered with the help of Teflon filter paper (0.45 μm). The filtrate thus obtained then re-precipitated in diethyl ether with powerful agitation and dispersed in methanol. Dissolved precipitates in methanol were dialyzed for 24 hours at 4 °C to remove organic solvent, freeze-dried and kept at −20 °C. For the synthesis of PCL-PEI-Fol copolymer, first 0.3 mM folate was activated using 1.2 mM NHS and 1.2 mM DCC similar to activation of PCL. 0.3 mM PCL-PEI was added in it and stirring continued for 4 hours. The mixture thus obtained was dialyzed using dialysis bag with MWCO 5000 at 4 °C for 48 hours, freeze dried and stored in freezer at −20 °C.

To obtain PCL-PEI-PEG copolymer, firstly glutaraldehyde-PEG (GA-PEG-GA) was prepared. For this purpose, 0.01 M PEG was taken in round bottom flask and refluxed for 24 hours at 40 °C while stirring at 150 rpm. After 24 hours, 0.1 M glutaraldehyde was added in the PEG solution and 10 mL of 1 M HCl was added, and mixture was stirred for 16 hours at ambient temperature. The reaction was then halted by adding 1 M NaOH in reaction mixture and stirring continued for 3 hours. The product thus obtained was dialyzed against distilled water for 24 hours, using dialysis bag (MWCO 1000). The solvent from resultant dispersion was removed completely using rotary evaporator. A sticky paste of GA-PEG-GA obtained and stored at −4 °C. Secondly, 0.27 mM PCL-PEI and 0.35 mM GA-PEG-GA solution in dichloromethane were prepared separately in conical flasks stirring vigorously. After 2 hours of continuous stirring GA-PEG-GA solution was added dropwise to PCL-PEI solution. The resultant mixture was stirred for 4 hours. Solvent was then evaporated to get viscous residue which was further dialyzed against deionized water at ambient temperature for 24 hours to remove any traces of solvent. Product thus obtained was concentrated using rotary evaporator. Dry powder of PCL-PEI-PEG obtained was stored at −4 °C.

### 2.3 Fabrication of nanoparticles–hydrogel drug delivery system

Precipitation method was used to prepare nanoparticles.[20] 0.3 g of PCL-PEI, PCL-PEI-PEG and PCL-PEI-Fol copolymers were taken in weight ratio 9%, 90% and 1% respectively and dissolved in 1 mL THF. The polymer solution thus attained was dropped slowly in 10 mL deionized water while slow stirring that was continued for 4 hours at ambient temperature. The solution thus obtained was dialyzed using dialysis membrane with MWCO 10 000 against deionized water for 12 hours. The nanoparticles thus obtained were stored at −4 °C. Drug loaded nanoparticles were prepared in the similar way. Doxorubicin was dissolved in polymer solution of PCL-PEI, PCL-PEI-PEG and PCL-PEI-Fol in 1 mL THF. Then, the solution was added dropwise in 10 mL deionized water. The obtained nanoparticles were dialyzed for 12 hours and stored at −4 °C for further characterizations.

For loading nanoparticles in hydrogel, 1.2% w/v chitosan solution was prepared. Nanoparticles and doxorubicin loaded nanoparticles were added separately to chitosan solution in weight ratio 1 : 20 and stirred slowly at 50 rpm for 2 hours so that homogeneous distribution of particles in hydrogel was obtained.

### 2.4 Physical characterization

Acid sensitive nanoparticle–hydrogel loses its mechanical integrity and deforms at low pH. The interaction between nanoparticles and hydrogel also weakens. It causes the instability of nanoparticles and nanoparticles agglomerate in static acidic environment. These phenomena were observed visually and recorded using camera. Concisely, nanoparticles loaded hydrogel samples were placed at pH 7.4 and 5.0 buffer solutions for 48 hours and observed the agglomeration of nanoparticles in hydrogel and mechanical stability of hydrogel by tilting the samples. The change in viscosity (sol–gel transition) at different pH values was measured by capillary rise method.[21] Nanoparticles–hydrogel samples were placed at normal physiological pH (7.4) and low pH (5.0). Capillary tubes with internal diameter of 0.3 mm were inserted vertically in both solutions and capillary rise in centimetres was measured at different time intervals.

### 2.5 Chemical characterization

The presence of representative functional groups in copolymers was investigated by Thermo Nicolet FTIR spectrophotometer (Nicolet 6700, Thermo scientific USA). Small amounts of PCL-PEI, PCL-PEI-Fol and PCL-PEI-PEG block polymers were taken and measured their FTIR spectra in the range of 4000–400 $cm^{-1}$. For studying the chemical makeup of copolymers, Broken MSL-300 spectrometer was utilized to get H-NMR spectra of copolymers. Tetramethylsilane and chloroform were used as internal standard and solvent respectively. The amount of folate attached with PCL-PEI copolymer was determined by Shimadzu UV-1280 spectrophotometer. Standard solutions of folate in serial dilution and PCL-PEI-Fol solution were prepared and recorded their spectra. Later, the attached quantity of folate in PCL-PEI-Fol was calculated by standard curve method.


© 2022 The Author(s). Published by the Royal Society of Chemistry

Open Access Article. Published on 02 November 2022. Downloaded on 11/13/2022 8:39:19 PM.
This article is licensed under a Creative Commons Attribution-NonCommercial 3.0 Unported Licence.

### 2.6 Particle size and zeta potential

Zetasizer Ultra (Malvern Panalytical, UK) was utilized to explore particle size (hydrodynamic diameter), PDI and particle charge of the nanoparticles. Distilled water was used to adjust specific concentration of nano-formulation. The analysis was carried out in triplicate; average was determined and described with standard deviation (SD).

To study the charge reversal characteristics of nanoparticles, phosphate buffer saline (PBS, 0.1 M) with pH 4.0, 6.4 and 7.4 were formulated. The nanoparticles were dispersed in 10 mL of buffer at each pH described above separately. The nanoparticles dispersions were then dialyzed using buffer of similar pH at 37 ° C for 6 h. Then, the dispersions from each dialyzing bag were poured out and their zeta potential were quantified by means of Zetasizer Ultra (Malvern Panalytical, UK). Each sample was analysed thrice, and average value was reported.

### 2.7 Morphological studies

Size, shape, and surface morphology of nanoparticles were visualized by JVEGA 3LMU, SANCO Scanning Electron Microscope. Small quantity of nanoparticles solution was placed on copper grid, dried, gold coated and observed under SEM at 10.0 kV accelerating voltage. The distribution of nanoparticles in chitosan hydrogel was assessed by transmission electron microscope (JEM-2100F, Japan). For TEM examination, the nanoparticles were stained with phosphotungstic acid and loaded in hydrogel. The sample was then diluted, dried a little portion on sample holder and examined under TEM.

### 2.8 Pharmacokinetic analysis

**2.8.1 Nanoparticles loading studies.** Nanoparticles loading efficiency of hydrogel was investigated by mass measurement. Briefly, certain quantity of nanoparticles loaded hydrogel was taken and washed with deionized water many times to get rid of unloaded nanoparticles from hydrogel. Later, the hydrogel was dispersed in tetrahydrofuran to extract nanoparticles from hydrogel. The suspension was centrifuged, supernatant was collected and dried to get loaded amount of nanoparticles in hydrogel. Finally, this amount was weighed and calculated the nanoparticles loading efficiency using the below equation:

$$\text{NPs loading efficiency } (\%) = \frac{\text{Weight of loaded NPs}}{\text{Total weight of NPs added}} \times 100 \quad (1)$$

**2.8.2 Drug loading studies.** Encapsulation efficiency is the quantity of drug captured in nanoparticles out of a certain quantity of drug added. It is percent efficiency of nanoparticles to encompass drug. Encapsulation efficiency was calculated using the following equations:

$$\text{Encapsulation efficiency } (\%) = \frac{\text{Amount of encapsulated drug}}{\text{Total amount of drug added}} \times 100 \quad (2)$$

Briefly, 3 mg of the nanoparticles were dissolved in DMSO and investigated at 480 nm with the help of UV-Visible Spectrophotometer (LAMBDA 1050, PerkinElmer, USA). Concentration of doxorubicin was determined with the help of calibration curve. Calibration curve was drawn at different dilutions of doxorubicin (5–50 μg $mL^{-1}$) using UV-Visible spectrophotometer (LAMBDA 1050, PerkinElmer, USA). Sample concentrations were plotted against the respective absorbance value. Straight line equation thus obtained from the graph was further utilized to determine drug concentration from the value of sample absorbance.

**2.8.3 Drug release studies.** Dialysis method was used to assess the release of drug from nanoparticles–hydrogel at pH 7.4 and pH 6. Dialysis bags of MWCO 1000 were chosen and 5 mg dox loaded nanoparticles–hydrogel was sealed in it. The bags were suspended in 50 ml of buffer solutions of pH 7.4 and 5.0 at specific pH at 37 °C temperature in shaking incubator at 50 rpm. 2 ml of samples were taken at specific time intervals and replaced with equal amounts of buffer solutions of similar pH. The samples were filtered and assessed for drug content using UV spectrophotometer (Shimadzu, Japan) at 485 nm in triplicate and mean values were reported.

**2.8.4 Nanoparticles release studies.** 1 ml of nanoparticle–hydrogel samples were placed in 1 ml of pH 7.4 and pH 5.0 buffer solutions and incubated at 37 °C under constant shaking at 50 rpm. The supernatant was taken after certain time intervals, centrifuged at 35 000 rpm for 20 minutes and washed with deionized water to remove free chitosan molecules. Then, supernatant was discarded, and pellet was dried and weighed. The percentage release of nanoparticles was calculated by below equation:

$$\%\ \text{release of NPs} = \frac{\text{Weight of released NPs}}{\text{Total weight of NPs loaded in hydrogel}} \times 100 \quad (3)$$

### 2.9 Biological evaluation

**2.9.1 Cell culture.** MCF-7 cells were cultured in Dulbecco's Modified Eagles Medium (DMEM) containing 10% fetal bovine serum and 1% penicillin/streptomycin. Incubator conditions were set at a temperature of 37 °C and 5% $CO_2$ and the appropriate humidity to provide the body's natural environment for cell growth. The cells sub-cultured once touched 80% confluence and passaged 2 times afore their usage in additional tests. All the cell lines used were tested for absence of mycoplasma, bacteria, yeast, and fungi.

**2.9.2 Cytotoxicity studies.** MCF-7 cells were seeded at a density of 10 000 cells per $cm^2$ in 96-well plate using DMEM medium containing 10% fetal bovine serum and 1% penicillin/streptomycin. Nanoparticles samples were sterilized using 0.22 μm syringe filters during all cell experiments. After 24 h incubation, samples with increasing concentrations of doxorubicin (25, 50 and 100 μg $mL^{-1}$) were added to each well. MTT essay is used to assess viability of cells once exposed to the

Open Access Article. Published on 02 November 2022. Downloaded on 11/13/2022 8:39:19 PM.
This article is licensed under a Creative Commons Attribution-NonCommercial 3.0 Unported Licence.

nanoparticles. Concisely, 10 μL MTT dye in 100 μl DMEM medium was introduced in each well after the removal of the nanoparticles samples. The cells then incubated at 37 °C for 24 h and absorbance of plates was computed at 550 nm using micro plate reader (SpectraMax M3, Molecular Devices, USA). Absorbance at above-mentioned wavelengths was also noted after 48 and 72 h of cell incubation. Cytotoxicity determined by deducting living cells number from the total number of cells in each well.

# 3. Results and discussion

## 3.1 Formulation of nanoparticles–hydrogel drug delivery system

Conjugation technique was used for the fabrication of amphiphilic diblock (PCL-PEI) and triblock polymers (PCL-PEI-Fol). Covalent binding of PCL to PEI involves the use of DCC and NHS, both of which used communally to conjugate –COOH comprising polymers with $-NH_2$ comprising polymers. The –COOH group of PCL was activated by DCC and NHS in THF at 4 °C. Thus, semi stable NHS ester of PCL was obtained that would further react with amine of PEI resulting in the formation of stable PCL-PEI.[22] Excess amount of PEI was used to prevent the bonding of PCL to both terminal amines of PEI. In this way, the formation of PCL-PEI-PCL was inhibited. Analogously, conjugation of folate with PCL-PEI was carried out resulting in formation of PCL-PEI-Fol. A two-stage reaction was carried out to create acid sensitive linkage between PEG and PCL-PEI. Initially, PEG was reacted with glutaraldehyde in acidic conditions to obtain intermediate product GA-PEG-GA. Upon addition of PCL-PEI conjugation reaction occur between GA-PEG-GA and PCL-PEI resulting in formation of PCL-PEI-PEG.

These amphiphilic copolymers such as PCL-PEI-PEG, PCL-PEI and PCL-PEI-Fol and were mixed in 90 : 9 : 1 proportion and prepared their nanoparticles. The obtained nanoparticles form core–shell structure containing hydrophobic core of PCL and hydrophilic PEG shell extending outside the nanoparticles. The outer hydrophilic PEG layer enhances the stability and stealthy characteristic of nanoparticles and inner PCL core acts as a reservoir for hydrophobic drugs.[20] Finally, nanoparticles were loaded in chitosan hydrogel. This hybrid structure enhances the structural stability and certain properties of nanoparticles such as prolonged drug release.[23] Furthermore, the nanoparticles–hydrogel drug delivery system possesses intermolecular interactions between nanoparticles and chitosan chains. In acidic environment, this interaction is reduced due to protonation of nanoparticles and chitosan chains (Fig. 2). Consequently, the mutual acid sensitive interaction between nanoparticles and chitosan makes it highly sensitive to external acidic pH, and fast release of drug was observed at low pH.

## 3.2 Chemical analysis of copolymers

The FTIR spectra of PCL-PEI, PCL-PEI-PEG, PCL-PEI-folate and chitosan are depicted in Fig. 3a. The characteristic peaks of carbonyl group at about 1730 $cm^{-1}$ and C–O–C at 1042 $cm^{-1}$, 1100 $cm^{-1}$ and 1240 $cm^{-1}$ related to PCL was present in all spectra of copolymers.[24,25] It indicates the coupling of PCL in

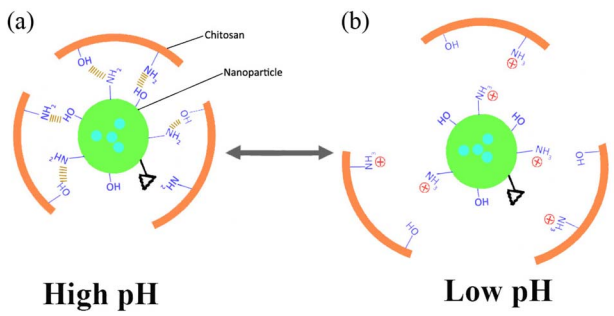



Fig. 2 Possible molecular interactions between nanoparticles and hydrogel (a) at high pH (structural stability due to hydrogen bonding) and (b) at low pH (disruption in molecular interactions).

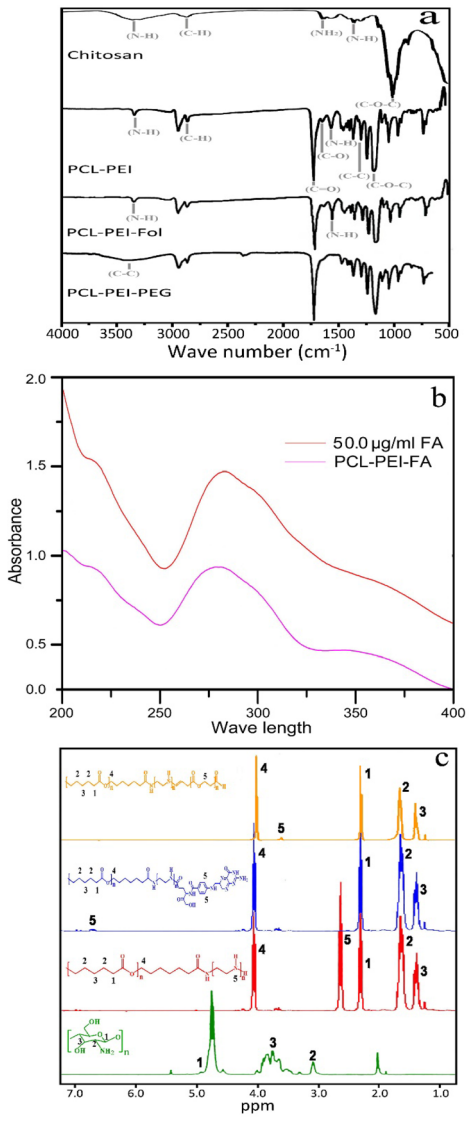



Fig. 3 FTIR spectra of hydrogel and copolymers (a), UV-visible spectra of PCL-PEI-Fol for the estimation of folate (b), and NMR spectra of hydrogel and copolymers.


© 2022 The Author(s). Published by the Royal Society of Chemistry

Open Access Article. Published on 02 November 2022. Downloaded on 11/13/2022 8:39:19 PM.
This article is licensed under a Creative Commons Attribution-NonCommercial 3.0 Unported Licence.

these copolymers. Peak at around 1220 $cm^{-1}$ conforms the N–H vibration of amines from PEI,[26] and hence showed its existence in PEI containing copolymers. Broad peak (3300–3600 $cm^{-1}$) of –OH from PEG was observed in PCL-PEI-PEG copolymer which depicts the conjugation of PEG in copolymers. Furthermore, a shoulder at about 1650 $cm^{-1}$ appeared in PCL-PEI-PEG copolymer attributes to imine bond[27] and validates the linkage between PEI and PEG.

The Investigation of folate coupling is well established using UV-visible spectroscopy.[28] PCL-PEI-FA solution give distinctive absorbance of folate at 280 nm (Fig. 3b) and the quantity of conjugated folate was determined using standard curve method. 93% of folate was cross-linked to PCL-PEI copolymer.

NMR was employed to further validate chemical makeup of copolymers. Representative peaks of PCL at 1.3, 1.5, 2.2 and 4.1 ppm[29] showed their presence in PCL-PEI, PCL-PEI-Fol and PCL-PEI-PEG copolymers. The PEG peak at 3.6 ppm describes the presence of ethylene glycol in PCL-PEI-PEG copolymer.[30] The peak of free hydrogen of amines from PEI was observed at 2.7 ppm in PCL-PEI. This peak disappears in PCL-PEI-Fol due to bonding with folate, and new peak of folate emerges at around 6.8 ppm.[20] In chitosan spectrum, peaks at 3.2, 3.7 and 4.9 ppm represent the hydrogens of glucosamine unit in chitosan.[31]

### 3.3 Hydrodynamic size and zeta potential

Amphiphilic triblock copolymers self-assemble in aqueous medium into hydrophobic core and hydrophilic shell. In aqueous medium, the hydrophilic chains of shell could extend out and surface groups such as PEG, PEI and folate are more exposed for interaction. Moreover, this phenomenon also increases the hydrodynamic size of nanoparticles, which could be calculated by dynamic light scattering (DLS).[19] The size and size distribution of nanoparticles were determined by DLS. Nanoparticles exhibited a unimodular distribution in aqueous medium. The average hydrodynamic size of the NPs was 238 nm as shown in Fig. 4a and 5.

To ascertain the charge reversal characteristic of nanoparticles in response to pH, zeta potential of nanoparticles was measured at different pH values. The nanoparticles demonstrated a negative zeta potential at pH 7.4. Conversely, a negative to positive change in zeta potential was observed at pH 6.0 as shown in Fig. 4b. The change in zeta potential from negative to positive established the generation of protonated PEI in acidic environment.[32] Additional reduction in the pH values led to increase in positive zeta potential of nanoparticles. The fact approved to the presence of additional amount of positively charged PEI in acidic medium. The negative to positive charge reversal implies that nanoparticles would have less interaction with normal body cells at physiological pH due to their negative surface potential, however appearance of positive surface potential when exposed to acidic environment of tumour augments the localization and strong interaction of nanoparticles with cancer cells. Furthermore, the increment in positive surface charges of nanoparticles at highly acidic

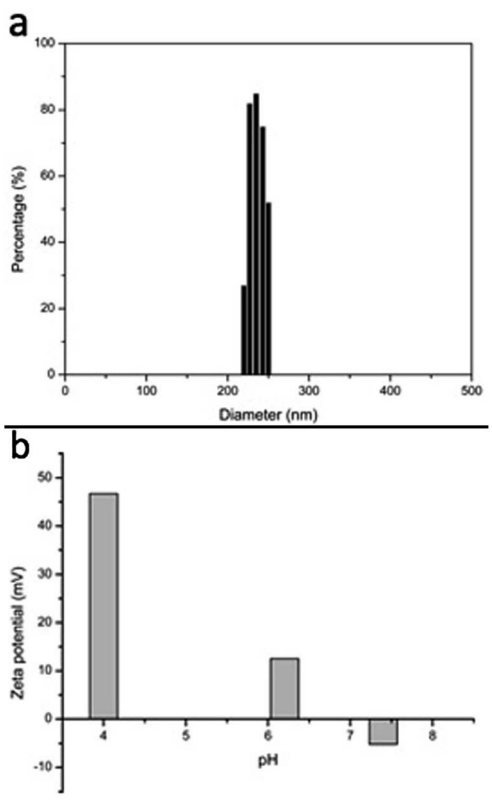



Fig. 4 Graphs of size calculation of nanoparticles using dynamic light scattering (a), and charge reversibility of nanoparticles observed at different pH values using zeta potential (b).

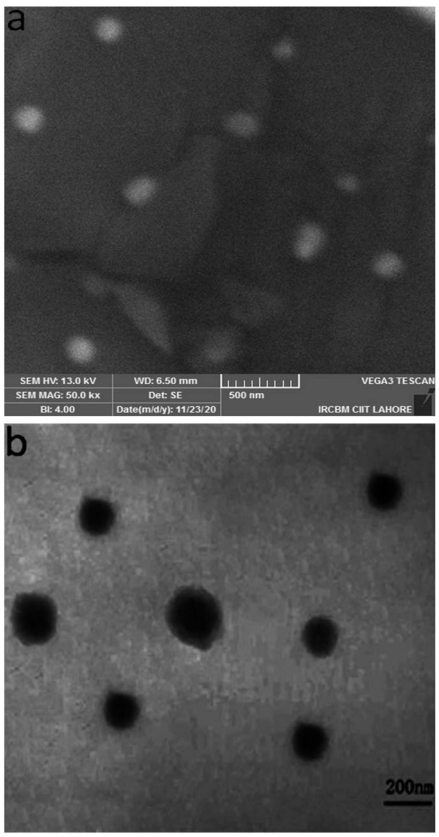



Fig. 5 SEM image of nanoparticles without loading in hydrogel (a), and TEM image nanoparticles after loading in hydrogel (2).

Open Access Article. Published on 02 November 2022. Downloaded on 11/13/2022 8:39:19 PM.
This article is licensed under a Creative Commons Attribution-NonCommercial 3.0 Unported Licence.

environment, such as lysosomal acidity (pH 4 and 5), would intensify the aptitude of these nanoparticles to escape from lysosomes owing to their proton sponge effect. Thus, they efficiently transport drug to cancer cells.[33]

### 3.4 Morphology and nanoparticles distribution

SEM was utilized to investigate the surface morphology and size of nanoparticles. The size of nanoparticles was found to be 150–200 nm. The size of nanoparticles between 50–200 nm is optimal for drug delivery to cancer. Some nanoparticles below 10 nm are filtered through kidney and nanoparticles bigger than 200 nm are eliminated through mononuclear phagocyte system.[34] SEM image shows stable spherical nanoparticles without any agglomeration. Nanoparticles display bright inner core and blurred outer layer; the inner core consists of hydrophobic PCL and outer shell is composed of hydrophilic PEG. These structural features of nanoparticles help in the stability of nanoparticles in body fluids.[35] Furthermore, the structural integrity and homogenous distribution of nanoparticles in hydrogel was further visualized by TEM. Dark spots of nanoparticles are homogenously distributed in hydrogels. Nanoparticles are stable in hydrogel and retained their shape and size (150–200 nm). The strong interactions between chitosan chains and nanoparticles could be the reason for good dispersion and minimum aggregation of nanoparticles in hydrogel.[36]

### 3.5 Stimuli responsiveness

Acidic environment responsive viscosity changes and agglomeration of nanoparticles in hydrogel were observed visually. The nanoparticles loaded hydrogel samples were placed in both acidic pH (6.0) and neutral pH (7.4) media for 24 hours and visualized the physical change. Upon tilting the samples, hydrogel of acidic media exhibited fluid behaviour. While hydrogel of neutral media showed gel-like behaviour (Fig. 6a). Since acid weakens the intermolecular interaction between chitosan chains, the hydrogel loses its gelation behaviour in acidic environment.[37] Furthermore, it was found that nanoparticles loaded hydrogel exhibited no agglomeration of nanoparticles in hydrogel when exposed to normal physiological pH. However, nanoparticles loaded hydrogel showed clearly visible aggregates of nanoparticles in hydrogel at acidic pH (Fig. 6b). This phenomenon occurs due to charge reversibility of nanoparticles; both nanoparticles and chitosan chains are protonated and get positive charges. Consequently, chitosan chains expel nanoparticles, and nanoparticles become unstable and aggregate in hydrogel. Overall, such characteristics of nanoparticles–hydrogel drug delivery system would facilitate the selective spreading of hydrogel, accumulation, and release of nanoparticles in tumour tissue.

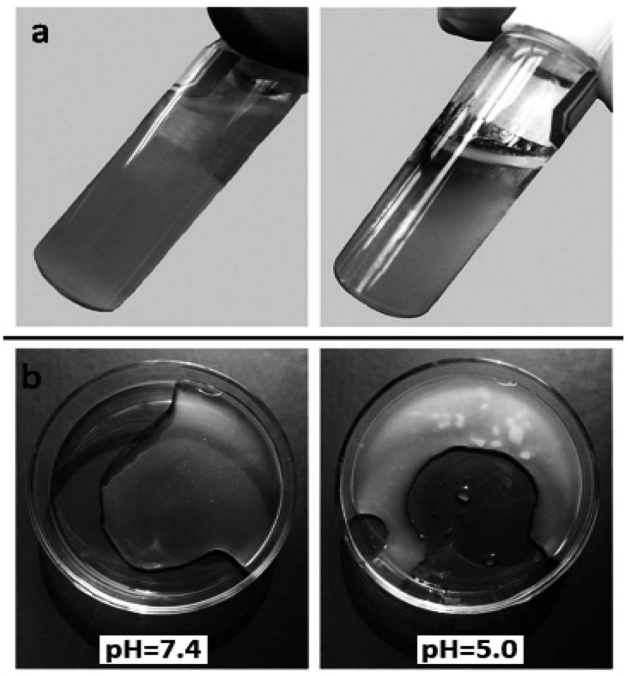



Fig. 6 Visual images of acidic environment responsive viscosity change (a), and agglomeration of nanoparticles at acidic pH (b).

### 3.6 Sol–gel transition and pharmacokinetic studies

The sol–gel transition of nanoparticles–hydrogel drug delivery system at acidic and neutral pH values was elaborated by capillary rise method. Clearly, the capillary rise of hydrogel in acidic environment is greater than that of normal environment. It implies that rate of gel-to-sol transition of hydrogel is fast in acidic environment and exhibited low pH responsive fluidity as compared to hydrogel in normal environment as shown in Fig. 7a. This acid susceptible gel-to-sol transition is beneficial for specific spreading of hydrogel in tumour tissue; the hydrogel would retain its jelly like structure in normal healthy environment of tissue and convert to fluid as it will sense tumour acidic environment.

The nanoparticles loading capacity of hydrogel was found to be 72%, which describes that nanoparticles are well enclosed within the polymeric chains of chitosan. The intermolecular interaction between amines and hydroxyl groups of nanoparticles and chitosan chains is the reason for good loading of nanoparticles in hydrogel.[38] Encapsulation efficiency of doxorubicin in nanoparticles was calculated by UV visible spectrophotometer and found to be 48%. Mostly doxorubicin is encapsulated inside the PCL core owing to its hydrophobic nature. High proportion of PCL-PEI-PEG was used in the nanoparticles to achieve maximum stability and encapsulation efficiency of nanoparticles. While small amount of PCL-PEI and PCL-PEI-Fol was utilized to add specific characteristics in nanoparticles.[20]

Different physical factors such as ionic strength, solvent polarity and pH can affect the nanoparticles suspension.[39] Nanoparticles could be released in specific media from hydrogel due to electrostatic repulsion. Release of nanoparticles from hydrogel was studied at both acidic pH (6.0) and normal pH (7.4). It was found that the nanoparticles are released from hydrogel in very less amount at normal pH (Fig. 7b). Nanoparticles possess negative surface charges at normal pH and hold efficient intermolecular interactions with chitosan chains


© 2022 The Author(s). Published by the Royal Society of Chemistry

Open Access Article. Published on 02 November 2022. Downloaded on 11/13/2022 8:39:19 PM.
This article is licensed under a Creative Commons Attribution-NonCommercial 3.0 Unported Licence.

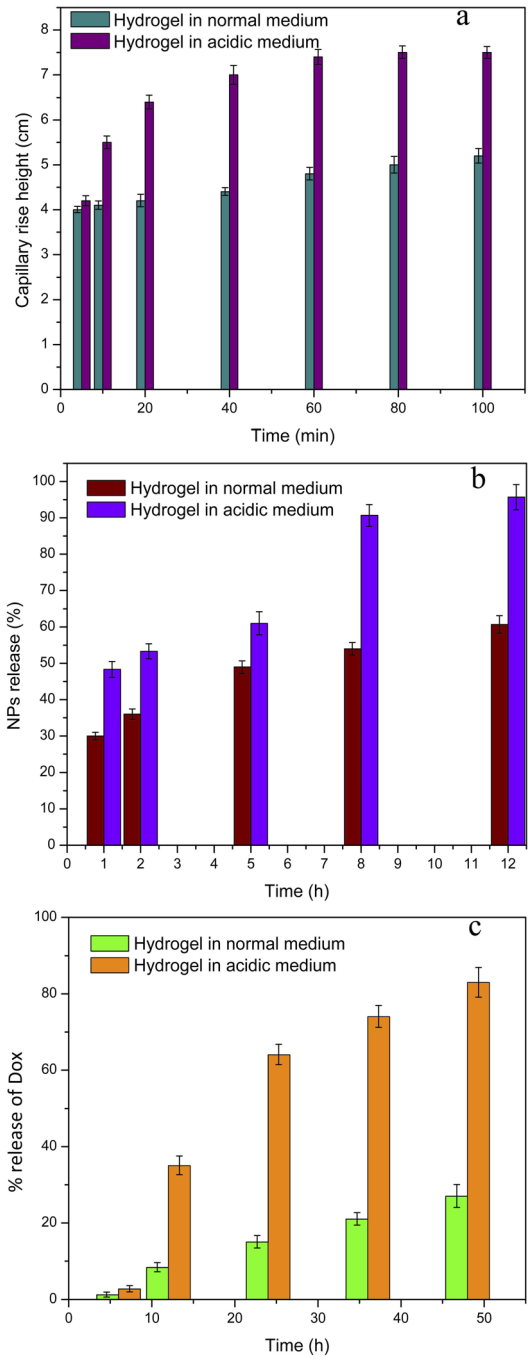



Fig. 7 Estimation of gel-to-sol transition of hydrogel in normal and acidic media through capillary rise method (a), release of nanoparticles from hydrogel in acidic and normal media (b), and release of drug from nanoparticles–hydrogel drug delivery system at normal and acidic media (c).

at neutral pH, which may hinder or slow down the release of nanoparticles from hydrogel.[40] However, release of nanoparticles at acidic pH is fast and more than 90% of nanoparticles were released in about 12 hours. The reasons for higher release of nanoparticles from hydrogel may be the unique behaviour of hydrogel and the nanoparticles in acidic environment. Both nanoparticles and chitosan chains get positive charges at acidic pH due to protonation of amines. Therefore, electrostatic repulsion causes the speedy release of nanoparticles from hydrogel. Another fact would be the change in viscosity of hydrogel at acidic pH; the hydrogel may swell with the rush of water inside acidic condition that would be responsible for greater release of nanoparticles due to diffusion phenomenon. The insertion of hydrogel in acidic environment of tumoral soft tissue would enhance the contact area between nanoparticles and tumour tissue. It would allow nanoparticles to diffuse into the tumour tissue from many sites. Thus, spatial distribution of the drug loaded nanoparticles within the tumour would increase resulting in higher concentration of drug at tumour site.

Very smaller amount of drug was released from nanoparticles at pH 7.4 which describes the stability of nanoparticles in normal physiological environment. Consequently, the nanoparticles are estimated to discharge a smaller amount of drug in healthy tissues and produce least side effects of drug in healthy cells. The PEGylation of nanoparticles plays a vital part to stabilize nanoparticles and extend retention time in body.[41] The extracellular environment of tumour contains acidic pH (<pH 7.4).[42] These nanoparticles demonstrated fast release of doxorubicin at low pH (6.0) as shown in Fig. 7c. Nanoparticles develop instability at low pH and release drug rapidly. Therefore, the concentration of doxorubicin in tumour tissues would augment to diffuse in cancer cells efficiently. If nanoparticles are engulfed by cancer cells as a result of endocytosis, they would be confined in endosomes where the pH is again very acidic.[43] Fortunately, the nanoparticles indicated improved release of doxorubicin at low pH. This increase in drug release would further enhance the accumulation of drug inside cancer cells to avert the normal cellular behaviour of cancer cells.

### 3.7 Biological studies

The increase in cancer cell viability in acidic environment provisions the concept that cancer cell line growth is improved

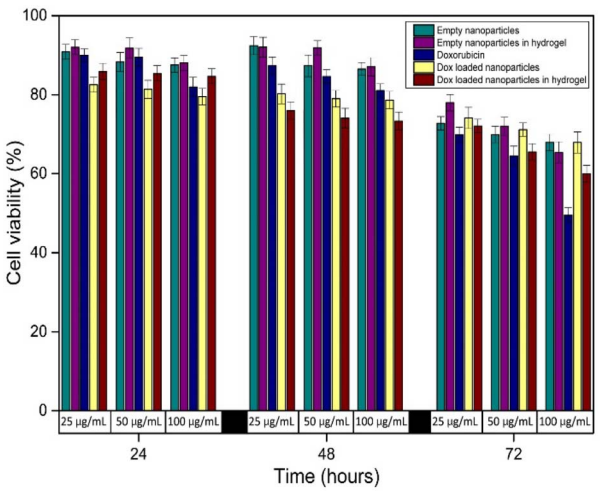



Fig. 8 Cell viability of nanoparticles–hydrogel drug delivery system and its components against MCF-7 cancer cell line at different time intervals.

Open Access Article. Published on 02 November 2022. Downloaded on 11/13/2022 8:39:19 PM.
This article is licensed under a Creative Commons Attribution-NonCommercial 3.0 Unported Licence.

in acidic environment.[44] In this work, MCF-7 breast cancer cell line was cultured in acidic medium to represent the tumour microenvironment and enhanced performance of acid sensitive nanoparticles–hydrogel drug delivery system. The cytotoxicity of empty nanoparticles, empty nanoparticles in hydrogel, doxorubicin loaded nanoparticles, doxorubicin loaded nanoparticles–hydrogel and free doxorubicin was assessed against MCF-7 cancer cell line. Three increasing concentrations were chosen and ascertained cell viability for three days respectively, as shown in Fig. 8. The anticancer effect of the doxorubicin loaded nanoparticles–hydrogel was significantly greater. It defines the specific targeting and entering of nanoparticles in cancer cells, and discharge of drug inside cells. The released doxorubicin would efficiently bind with DNA to prevent macromolecular biosynthesis and subsequently damage of cancer cells.[45] Conversely, free drug meets many cellular barriers to reach at its active site within cancer cell.[46] But in *in vitro* studies, the free doxorubicin would be easily infused into growth medium and cancer cells compared to the drug enclosed in the nanoparticles and hydrogel. Thus, free doxorubicin exhibited more toxicity against MCF-7 cells as compared to doxorubicin loaded nanoparticles–hydrogel system. Furthermore, the reduction in cell viability with reference to time and concentration endorses the sustained slow release of doxorubicin from nanoparticles and nanoparticles–hydrogel system. The sustained release of drugs from nanoparticles–hydrogel system would be favourable to inhibit the proliferation of cancer cells for elongated time.[47] Remarkably, empty nanoparticles and nanoparticles–hydrogel also displayed slight toxicity against MCF-7 cancer cells due to the presence of positive surface charges on nanoparticles and hydrogel in acidic environment. This appearance of positive charges produces toxicity in nanoparticles in acidic milieu owing to their robust interaction and distraction of cell membranes.[48]

## Conclusions

In this study nanoparticles incorporated hydrogel was developed for localized drug delivery to cancer. We prepared pH responsive polymeric nanoparticles and loaded in chitosan hydrogel. SEM, TEM and DLS studies describe the unimodular distribution of round nanoparticles in hydrogel. The drug encapsulation and nanoparticles loading efficiencies were obtained as 48% and 72% respectively which describes the better physicochemical interactions among drug, nanoparticles, and hydrogel matrix. Zeta potential, viscosity measurements and drug/nanoparticles release studies confirmed the pH responsive behaviour of nanoparticles and hydrogel. It facilitates the good packing of drug in physiological environment and quick release of drug/nanoparticles in acidic cancer environment. MTT assay further confirmed the better anticancer effect of nanoparticles incorporated hydrogel as compared to free drug or free drug loaded nanoparticles. Overall, this nanoparticles–hydrogel hybrid drug delivery system could be utilized for regional chemotherapy.

## Conflicts of interest

There are no conflicts to declare.

## Acknowledgements

This research was supported by Higher Education Commission, Pakistan under start-up research grant (IPFP/HRD/HEC/2015/680) and COMSATS University Islamabad under COMSATS research grant program (16-49/CRGP/CIIT/LHR/16/1184). We are grateful to Higher Education Commission for providing fellowship to PhD scholar under Indigenous PhD Fellowship for 5000 Scholars (Phase-II).

## References

1 M. Höglund, D. Gisselsson, N. Mandahl, B. Johansson, F. Mertens, F. Mitelman and T. Säll, *Genes, Chromosomes Cancer*, 2001, **31**, 156–171.
2 S. R. Wolman, *Cancer Metastasis Rev.*, 1983, **2**, 257–293.
3 Z. Liu, K. Chen, C. Davis, S. Sherlock, Q. Cao, X. Chen and H. Dai, *Cancer Res.*, 2008, **68**, 6652–6660.
4 A. I. Minchinton and I. F. Tannock, *Nat. Rev. Cancer*, 2006, **6**, 583–592.
5 S. Nagano, J. Y. Perentes, R. K. Jain and Y. Boucher, *Cancer Res.*, 2008, **68**, 3795–3802.
6 J. A. Dowell, A. R. Sancho, D. Anand and W. Wolf, *Adv. Drug Delivery Rev.*, 2000, **41**, 111–126.
7 D. Ding, Z. Zhu, R. Li, X. Li, W. Wu, X. Jiang and B. Liu, *ACS Nano*, 2011, **5**, 2520–2534.
8 B. Bahmani, H. Gong, B. T. Luk, K. J. Haushalter, E. DeTeresa, M. Previti, J. Zhou, W. Gao, J. D. Bui and L. Zhang, *Nat. Commun.*, 2021, **12**, 1–12.
9 M. Norouzi, B. Nazari and D. W. Miller, *Drug Discovery Today*, 2016, **21**, 1835–1849.
10 N. A. Peppas and A. S. Hoffman, in *Biomaterials science*, Elsevier, 2020, pp. 153–166, DOI: DOI: **10.1016/B978-0-12-816137-1.00014-3**.
11 N. Bhattarai, J. Gunn and M. Zhang, *Adv. Drug Delivery Rev.*, 2010, **62**, 83–99.
12 M. Dash, F. Chiellini, R. M. Ottenbrite and E. Chiellini, *Prog. Polym. Sci.*, 2011, **36**, 981–1014.
13 T. T. Dang, A. V. Thai, J. Cohen, J. E. Slosberg, K. Siniakowicz, J. C. Doloff, M. Ma, J. Hollister-Lock, K. M. Tang and Z. Gu, *Biomaterials*, 2013, **34**, 5792–5801.
14 B. Gao, J. Luo, Y. Liu, S. Su, S. Fu, X. Yang and B. Li, *Int. J. Nanomed.*, 2021, **16**, 4073.
15 A. Almeida, M. Araújo, R. Novoa-Carballal, F. Andrade, H. Gonçalves, R. L. Reis, M. Lúcio, S. Schwartz Jr and B. Sarmento, *Mater. Sci. Eng., C*, 2020, **112**, 110920.
16 S. Merino, C. Martin, K. Kostarelos, M. Prato and E. Vazquez, *ACS Nano*, 2015, **9**, 4686–4697.
17 W. Gao, Y. Zhang, Q. Zhang and L. Zhang, *Ann. Biomed. Eng.*, 2016, **44**, 2049–2061.
18 H. Derakhshankhah, R. Jahanban-Esfahlan, S. Vandghanooni, S. Akbari-Nakhjavani, B. Massoumi, B. Haghshenas, A. Rezaei, A. Farnudiyan-Habibi,


© 2022 The Author(s). Published by the Royal Society of Chemistry

Open Access Article. Published on 02 November 2022. Downloaded on 11/13/2022 8:39:19 PM. This article is licensed under a Creative Commons Attribution-NonCommercial 3.0 Unported Licence.

H. Samadian and M. Jaymand, *J. Appl. Polym. Sci.*, 2021, **138**, 50578.
19 A. Ahmed, S. Liu, Y. Pan, S. Yuan, J. He and Y. Hu, *ACS Appl. Mater. Interfaces*, 2014, **6**, 21316–21324.
20 A. Shahzadi, F. Ikram, R. U. H. Subhani, A. Ahmed, A. Asif, N. Fatima, A. A. Chaudhry and Y. Hu, *Int. J. Polym. Mater.*, 2020, **69**, 1187–1196.
21 W. Xu, H. Tang, H. Lv, J. Li, X. Zhao, H. Li, N. Wang and X. Yang, *Soft Matter*, 2012, **8**, 726–733.
22 J. Zhao, G. Weng, J. Li, J. Zhu and J. Zhao, *Mater. Sci. Eng., C*, 2018, **92**, 983–994.
23 M. Åhlén, G. K. Tummala and A. Mihranyan, *Int. J. Pharm.*, 2018, **536**, 73–81.
24 C. O. Silva, P. Rijo, J. Molpeceres, I. V. Figueiredo, L. Ascensão, A. S. Fernandes, A. Roberto and C. P. Reis, *Int. J. Pharm.*, 2015, **493**, 271–284.
25 E. Abdelrazek, A. Hezma, A. El-Khodary and A. Elzayat, *Egypt. J. Basic Appl. Sci.*, 2016, **3**, 10–15.
26 B. Wang, T. P. Huynh, W. Wu, N. Hayek, T. T. Do, J. C. Cancilla, J. S. Torrecilla, M. M. Nahid, J. M. Colwell and O. M. Gazit, *Adv. Mater.*, 2016, **28**, 4012–4018.
27 D. Xiao, H. Z. Jia, J. Zhang, C. W. Liu, R. X. Zhuo and X. Z. Zhang, *Small*, 2014, **10**, 591–598.
28 A. Hashemian, H. Eshghi, G. Mansoori, A. Shakeri-Zadeh and A. Mehdizadeh, *Int. J. Nanosci. Nanotechnol.*, 2009, **5**, 25–34.
29 H. Chen, S.-Y. Lee and Y.-M. Lin, *Polymers*, 2020, **12**, 1500.
30 B. Jeong, M. R. Kibbey, J. C. Birnbaum, Y.-Y. Won and A. Gutowska, *Macromolecules*, 2000, **33**, 8317–8322.
31 A. Geçer, N. Yıldız, A. Çalımlı and B. Turan, *Macromol. Res.*, 2010, **18**, 986–991.
32 J. Hu, S. Miura, K. Na and Y. H. Bae, *J. Controlled Release*, 2013, **172**, 69–76.
33 I. Richard, M. Thibault, G. De Crescenzo, M. D. Buschmann and M. Lavertu, *Biomacromolecules*, 2013, **14**, 1732–1740.
34 N. Hoshyar, S. Gray, H. Han and G. Bao, *Nanomedicine*, 2016, **11**, 673–692.
35 T. Limongi, M. Canta, L. Racca, A. Ancona, S. Tritta, V. Vighetto and V. Cauda, *Nanomedicine*, 2019, **14**, 797–801.
36 G. Bovone, E. A. Guzzi, S. Bernhard, T. Weber, D. Dranseikiene and M. W. Tibbitt, *Adv. Mater.*, 2022, **34**, 2106941.
37 K. Yang, H. Dang, L. Liu, X. Hu, X. Li, Z. Ma, X. Wang and T. Ren, *Int. J. Biol. Macromol.*, 2019, **141**, 876–884.
38 T. K. Giri, A. Thakur, A. Alexander, H. Badwaik and D. K. Tripathi, *Acta Pharm. Sin. B*, 2012, **2**, 439–449.
39 Z. Jin, Y. Mantri, M. Retout, Y. Cheng, J. Zhou, A. Jorns, P. Fajtova, W. Yim, C. Moore and M. Xu, *Angew. Chem., Int. Ed.*, 2022, **61**, e202112995.
40 T. Chen, K. Hou, Q. Ren, G. Chen, P. Wei and M. Zhu, *Macromol. Rapid Commun.*, 2018, **39**, 1800337.
41 J. S. Suk, Q. Xu, N. Kim, J. Hanes and L. M. Ensign, *Adv. Drug Delivery Rev.*, 2016, **99**, 28–51.
42 Y. Hao, C. Zheng, L. Wang, Y. Hu, H. Guo, Q. Song, H. Zhang, Z. Zhang and Y. Zhang, *J. Mater. Chem. B*, 2017, **5**, 2133–2144.
43 E. Oude Blenke, M. Sleszynska, M. Evers, G. Storm, N. Martin and E. Mastrobattista, *Bioconjugate Chem.*, 2017, **28**, 574–582.
44 V. A. Sethuraman, M. C. Lee and Y. H. Bae, *Pharm. Res.*, 2008, **25**, 657–666.
45 O. Tacar, P. Sriamornsak and C. R. Dass, *J. Pharm. Pharmacol.*, 2013, **65**, 157–170.
46 S. Kim, Y. Shi, J. Y. Kim, K. Park and J.-X. Cheng, *Expert Opin. Drug Delivery*, 2010, **7**, 49–62.
47 G. Zhao, L. Long, L. Zhang, M. Peng, T. Cui, X. Wen, X. Zhou, L. Sun and L. Che, *Sci. Rep.*, 2017, **7**, 1–10.
48 R. B. Arote, T. H. Kim, Y. K. Kim, D. Jere, H. L. Jiang, I. Y. Park, M. H. Cho, J. W. Nah and C. S. Cho, *Key Eng. Mater.*, 2007, **342**, 453–456.

© 2022 The Author(s). Published by the Royal Society of Chemistry